Influence of biotin lipid surface density and accessibility on avidin binding to the tip of an optical fiber sensor

ARTICLE *in* LANGMUIR · NOVEMBER 1992

Impact Factor: 4.46 · DOI: 10.1021/la00047a034

2 AUTHORS, INCLUDING:

Wiliiam M Reichert
Duke University
60 PUBLICATIONS **3,100** CITATIONS

Influence of Biotin Lipid Surface Density and Accessibility on Avidin Binding to the Tip of an Optical Fiber Sensor

Shulei Zhao† and W. M. Reichert*

Department of Biomedical Engineering and the Center for Emerging Cardiovascular Technologies, Duke University, Durham, North Carolina 27701

Received July 10, 1992

LB films doped with biotin lipids were deposited at the tip of an evanescent fiber optic (EFO) sensor, and the fluorescence intensity of FITC-labeled avidin bound to the sensor tip was monitored. The influence of receptor density and receptor surface accessibility on avidin binding to, and desorption from, the sensor surface was investigated. This was accomplished by varying the doping density from 0 to 100 mol % of two biotinylated phosphatidylethanolamines B-DPPE and B-X-DPPE, where B-X-DPPE is essentially identical to B-DPPE, except B-X-DPPE has a six carbon amino acid spacer interposed between the DPPE and the biotin hapten. In general, increasing the biotin lipid surface density or the biotin hapten accessibility increased both the affinity and amount of avidin bound to the sensor tip. Increasing the biotin lipid doping density also hastened the binding of avidin to a relatively inaccessible B-DPPE hapten, but slowed the binding of avidin to the more accessible B-X-DPPE hapten. Overall, avidin bound to the biotin-doped sensor surface 3–4 orders of magnitude slower and dissociated from the sensor surface considerably faster than that observed for avidin/biotin binding and dissociation in solution, particularly at low biotin doping densities. These observations suggest a sterically hindered binding of avidin to the biotin lipids at the sensor surface.

Introduction

Specific protein binding to receptors at cell membrane surfaces is common to a broad range of cellular functions like cell growth and differentiation, immune cell recognition and response, and neurotransmitter function.[1] An important aspect of studying these phenomena is devising a scheme for examining protein interactions with model membranes of known receptor composition. Ringsdorf and co-workers have reviewed how a fluorescence microscope configured with a "mini" Langmuir trough can be used to study specific protein binding to lipid monolayers at the gas/liquid interface.[2] Hafeman et al. introduced supported lipid monolayers to study the interactions between macrophages and haptens in model membranes.[3] Tamm and McConnell extended this technique to produce lipid bilayers to study the interaction of proteins with supported bilayer membranes constructed at the solid/liquid interface.[4] Thompson and co-workers have reviewed the Langmuir–Blodgett (LB) deposition of these model membrane structures and the fluorescence microscopy techniques suitable for studying them.[5,6] In her own work, Thompson and co-workers have used total internal reflection fluorescence microscopy (TIRFM) to study the interaction of proteins with supported bilayer membranes.[6] TIRFM is well suited for this purpose because it uses the evanescent wave on the liquid side of the solid/liquid interface to excite fluorescence to a depth of only a few tenths of a micrometer into the liquid phase.[7]

Receptor-containing lipid membranes have also been proposed as chemically selective layers for technical applications. Potential applications range from biomimetic transduction mechanisms for biosensing[8] to affinity-based drug delivery techniques.[9] It also has been proposed that receptor-doped, LB deposited, membranes at the tip of an evanescent fiber optic sensor (EFO) could be suitable for performing remote and targeted protein binding.[10] As discussed in detail elsewhere,[11] EFO sensors, like TIRFM, detect fluorescence generated only at the solid/liquid interface, but much more simply, conveniently, and efficiently. However, unlike TIRFM, EFO sensors lack the ability to spatially resolve fluorescence images.

Recently, we used an EFO system to demonstrate the specific binding of the protein avidin to monolayers of arachidic acid (AA) doped with a biotinylated phospholipid.[12] AA was selected as the matrix lipid for the sensor work because it is readily deposited onto the small and cylindrical surface of an optical fiber core using the LB technique,[13] whereas phospholipids are comparatively more difficult to deposit even on the most straightforward of geometries.[5] The commercially available avidin/biotin lipid system was selected as the ligand/receptor pair owing

* Author to whom correspondence should be addressed.
† Current address: Department of Ophthalmology & Visual Science, Yale University School of Medicine, New Haven, CT 06510.

(1) Darnell, J.; Lodish, H.; Baltimore, D. *Molecular Cell Biology*; Scientific American Books: New York, 1990.
(2) Ahlers, M.; Müller, W.; Reichert, A.; Ringsdorf, H.; Venzmer, J. Specific Interactions of Proteins with Functional Lipid Monolayers-Ways of Simulating Biomembrane Processes. *Angew. Chem., Int. Ed. Engl.* **1990**, *29*, 1269–1285.
(3) Hafeman, D. G.; von Tscharner, V.; McConnell, H. M. Specific Antibody-Dependent Interactions between Macrophages and Lipid Haptens in Planar Lipid Monolayers. *Proc. Natl. Acad. Sci. U.S.A.* **1981** *78*, 4552–4556.
(4) Tamm, L. K.; McConnell, H. M. Supported Phospholipid Bilayers. *Biophys. J.* **1985**, *47*, 105–113.
(5) Thompson, N. L.; Palmer, A. G., III. Model Cell Membranes on Planar Substrates. *Comments Mol. Cell. Biophys.* **1988**, *5*, 39–56.
(6) Thompson, N. L.; Palmer, A. G., III; Wright, L. L.; Scarborough, P. E. Fluorescence Techniques for Supported Planar Model Membranes. *Comments Mol. Cell. Biophys.* **1988**, *5*, 109–131.
(7) Reichert, W. M. Evanescent Detection of Adsorbed Films: Assessment of Optical Considerations for Absorbance and Fluorescence Spectroscopy at Crystal/Solution and Polymer/Solution Interfaces. *Crit. Rev. Biocompat.* **1989**, *5*, 173–205.
(8) Krull, U. J.; Thompson, M. The Lipid Membrane as a Selective Chemical Transducer. *IEEE Trans. Electron Devices* **1985**, *ED-32*, 1180–1184.
(9) Klibanov, A. L.; Bogdahov, A. A.; Torchilin, V. P.; Huang, L. Biotin-Bearing pH Sensitive Liposomes: high-affinity binding to avidin layer. *J. Liposome Res.* **1989**, *1*, 233–244.
(10) Reichert, W. M.; Brukner, C. J.; Joseph, J. Langmuir-Blodgett Films and Black Lipid Membranes in Biospecific Surface Selective Sensors. *Thin Solid Films* **1987**, *152*, 345–376.
(11) Thompson, R. B.; Ligler, F. S. Chemistry and Technology of Evanescent Wave Biosensors. In *Biosensors with Fiberoptics*; Wise, D. L., Wingard, L. B., Eds.; 1991; pp 111–138.
(12) Zhao, S.; Reichert, W. M. Langmuir-Blodgett Affinity Surfaces: targeted binding of avidin to biotin-doped Langmuir-Blodgett films at the tip of an optical fiber sensor. In *Macromolecular Assemblies in Polymeric Systems*; Stroeve, P., Balazs, A. C., Eds.; ACS Symposia Series 493; American Chemical Society: Washington, DC, 1992; pp 122–134.
(13) Zhao, S.; Reichert, W. M. Modeling of Fluoresence Emission from Cyanine-Dye-Impregnated Langmuir-Blodgett Films Deposited on the Surface of an Optical Fiber. *Thin Solid Films* **1991**, *200*, 363–373.

0743-7463/92/2408-2785$03.00/0

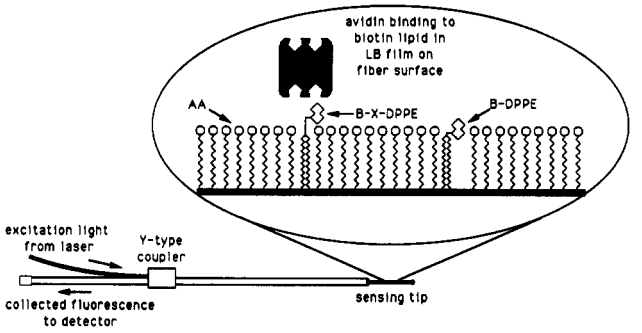

Figure 1. Schematic illustration of the evanescent fiber optic sensor configuration used to excite and collect fluorescence of surface bound FITC-labeled avidin. Blown up section of fiber tip shows orientation of LB film deposited on fiber surface. Note the different degrees to which B-DPPE and B-X-DPPE extend their biotin groups into the aqueous phase.

to its high binding affinity ($\sim 10^{15}\ M^{-1}$), broad technological applications, and high level characterization.[14]

In the current paper we investigate the influence of receptor density and receptor accessibility on avidin binding to, and desorption from, an EFO sensor deposited with LB films of AA doped with 0–100 mol % lipid receptors. The lipid receptors used in these measurements were two biotinylated phosphatidylethanolamines: B-DPPE or B-X-DPPE. The biotin lipid B-X-DPPE is essentially identical to B-DPPE, except that is has a six-carbon amino acid spacer interposed between the DPPE and the biotin hapten.[15] Codeposition of AA with B-DPPE and B-X-DPPE produced the LB films schematically illustrated in Figure 1. From published values of bond lengths and bond angles,[16] we estimate that the entire B-DPPE lipid has a molecular length that is just slightly longer (~2–5 Å) than the arachidic acid matrix lipid (~23 Å), with the hapten group of B-DPPE protruding just slightly above the surface of the AA film. B-X-DPPE was similarly estimated be 11–14 Å longer than an arachidic acid molecule, thus placing the biotin hapten above the surface of the AA film. However, note that none of the LB films deposited on the fiber tip contained both B-DPPE and B-X-DPPE as suggested by Figure 1.

In general, we observed that increasing the biotin lipid doping density and biotin hapten accessibility increased both the affinity and amount of avidin binding to the sensor tip. In addition, increasing the biotin lipid doping density hastened the binding of avidin to a relatively inaccessible B-DPPE hapten but slowed the binding of avidin to the more accessible B-X-DPPE hapten. However, in comparison to avidin/biotin binding in solution,[17] avidin binding to the biotin-doped sensor surface was 3–4 orders of magnitude slower, particularly at low biotin doping densities. Overall, it appears that the initial binding of avidin to the sensor surface was subject to considerable steric hindrance, but the long term stability of the surface-bound complex was augmented by higher doping densities that encouraged bivalent avidin binding to the sensor surface.

Experimental Section

EFO Sensor Fabrication. All avidin binding and desorption experiments were performed using an evanescent fiber optic (EFO) sensor in the fluorescence spectroscopy mode. Each sensor consisted of two step-index, quartz optical fibers (Quartz Products Corp.): a 600-μm sensing fiber and a 200-μm laser delivery fiber. The plastic jacket and cladding of the fiber were stripped from the distal end and the midsection of the of the sensing fiber and the distal end of the excitation fiber. The distal end of the sensing fiber was configured into an epoxy capped evanescent sensing tip, and the distal end of the excitation fiber was fused to the midsection of the sensing fiber to form an EFO sensor with a Y-type optical coupler (Figure 1). Detailed descriptions of the sensor fabrication and characterization are available elsewhere.[12] The epoxy capped fiber tip was immersed in a 10% (v/v) dimethyldichlorosilane (DDS, Sigma) in toluene (Aldrich) for 20 min and then rinsed sequentially with methanol, distilled water, and again methanol. This final step was necessary to "hydrophobize" the fiber surface so that a head-group-out oriented LB monolayer could be deposited at the sensor tip (Figure 1).

Deposition of Biotinylated LB Monolayers. The amphiphiles used in this study were arachidic acid (AA, Kodak) and the biotinylated phospholipids *N*-(biotinoyl)dipalmitoyl-L-α-phosphatidylethanolaminetriethylammonium salt (B-DPPE, Molecular Probes) and *N*-(6-((biotinoyl)amino)hexanoyl]dipalmitoyl-L-α-phosphatidylethanolaminetriethylammonium salt (B-X-DPPE, Molecular Probes). Stock solutions (1.2 and 1.0 mg/mL, respectively) of AA and the biotin lipids were made in chloroform (Fischer) and combined in precise amounts to produce various spreading solutions as listed in Table I. Thirty microliters of spreading solution was deposited dropwise on the surface of distilled–deionized water in an LB film balance (NIMA). After allowing 15 min for equilibration, the film was slowly compressed to a pressure of 35 mN/m and a monolayer was deposited on the silane-treated fiber tip during the downstroke. Figure 1 contains a schematic illustration of the head-group-out oriented monolayer deposited on the sensor tip (note that both biotin lipids are pictured for comparison, but none of the films contained both B-DPPE and B-X-DPPE). Calculations of transfer ratio of fatty acid onto the fiber tip (0.9) and estimates of the deposited film quality using this configuration are discussed in detail elsewhere.[13] The monolayer-coated fiber tip was then configured into a simple flow cell apparatus without removing the fiber tip from aqueous solution. The fiber tip/flow cell assembly was then used for the binding measurements. Total volume of the flow cell was approximately 1 mL. A detailed description of the LB film deposition and flow cell configuration is available elsewhere.[12]

Avidin Binding Experiments. Fluorescein isothiocyanate (FITC) labeled avidin (FITC-avidin, Sigma) with an average of 3.9 labels per protein molecule was dissolved without further purification in 0.01 M phosphate buffered saline (PBS, pH 7.5) with 0.5 M NaCl concentration. FITC-avidin solutions were used for the B-DPPE (10 μg/mL) and B-X-DPPE (5 μg/mL) binding experiments. High ionic strength PBS (0.5 M NaCl) was used to reduce nonspecific adsorption of avidin to the sensor surface.[18] Fluorescence was excited with the 488-nm line of an air-cooled Ar ion laser (Ion Laser Technologies) and collected from 490 to 600 nm at 5-nm intervals. After the fiber tip was assembled into the flow cell, the residual water in the flow cell was displaced with PBS followed by collection of a background signal (B_1). Next, 5 mL of protein solution was infused into the flow cell to displace the buffer. Starting with the initiation of protein infusion ($t = 0$), fluorescence intensity was collected at increasing time intervals for a minimum of 60 min. The difference between the collected fluorescence intensity (S_1) and the PBS background (B_1) was the fluorescence intensity attributed to the fluorescently-labeled avidin bound on the sensor surface ($F_1 = S_1 - B_1$).

Avidin Desorption Experiments. Avidin desorption was measured on eight sensor tips with LB monolayers doped with either B-DPPE or B-X-DPPE at 0.4, 0.99, 6.25, and 16.7 mol %. After monolayer deposition and flow cell assembly and PBS flushing, 5 mL of 20 μg/mL FITC-avidin was infused into the flow cell volume. FITC-avidin was allowed to adsorb to the sensor surface for 30 min, followed by flushing the flow cell with 15 mL of PBS and then infusing 5 mL of 100 μg/mL D-biotin (Sigma)

(14) Wilchek, M.; Bayer, E. A., Ed. Avidin-Biotin Technology. *Methods Enzymol.* **1990**, *184*.
(15) Haugland, R. P. *Handbook of Fluorescent Probes and Research Chemicals*; Molecular Probes, Inc.: Eugene, OR, 1989.
(16) *Handbook of Physics and Chemistry*; CRC Press: Cleveland, OH, 1974; Vol. 54.
(17) Green, N. M. Avidin 1: The Use of [^{14}C] Biotin for Kinetic Studies and for Assay. *Biochem. J.* **1963**, *89*, 585–591.
(18) Duhamel, R. C.; Whitehead, J. S. *Methods Enzymol.* **1990**, *184*, 201–207.

Table I. Biotin Lipid Content of LB Films Deposited at Fiber Tip

AA and biotin lipid composition of spreading solution		biotin lipid surface density of LB film[b]		estimated biotin lipids consumed per surface bound avidin molecule[c]
AA to biotin lipid ratio[a]	mol % biotin lipid	10^{12} lipids/cm^2	10^{-11} mol/cm^2	
1:0	0.00	0.00	0.00	0.0:1
600:1	0.17	0.93	0.15	0.3:1
350:1	0.28	1.58	0.26	0.5:1
250:1†	0.40	2.20	0.37	0.7:1
200:1	0.50	2.75	0.46	0.8:1
158:1	0.63	3.47	0.58	1.1:1
130:1	0.76	4.20	0.70	1.3:1
100:1†	0.99	5.43	0.90	1.7:1
70:1	1.41	7.69	1.27	2.3:1
55:1	1.79	9.71	1.61	2.9:1
45:1	2.17	11.8	1.95	3.6:1
36:1	2.70	14.5	2.41	4.4:1
30:1	3.23	17.2	2.86	5.2:1
20:1	4.76	25.0	4.15	7.6:1
15:1†	6.25	32.3	5.36	9.8:1
5:1†	16.7	76.9	12.8	23.3:1
0:1	100	250	41.5	75.8:1

[a] † indicates doping densities used in both binding and desorption experiments. [b] Assumes transfer ratio of 1.0. 20 Å^2/molecule for AA and 40 Å^2/molecule for biotin lipid. [c] 3025 Å^2/molecule for avidin (i.e. 3.3×10^{11} molecules/cm^2).

in PBS. The relatively high concentration of D-biotin remained in the flow cell through out the desorption experiment to prevent reattachment of desorbed avidin to the sensor surface. Fluorescence intensity was collected immediately after the infusion of the D-biotin and periodically during the 4–11 days that the desorption experiments were conducted. The loss of biotin lipid from the sensor surface was estimated at the end of each desorption experiment by rinsing the flow cell with 15 mL of PBS, followed by infusing another 5 mL of 20 μg/mL FTIC-avidin. After allowing 30 min for avidin rebinding to the sensor surface, 5 mL of 100 μg/mL D-biotin was introduced into the flow cell, followed by a final measure of fluorescence intensity (F_e'). The ratio F_e'/F_e provided a fractional measure of the biotin lipid conserved throughout each desorption experiment. The average value for this measurement was $F_e'/F_e = 0.92$ (±0.16%).

Relative Fluorescence Intensity. At the end of each avidin binding or desorption experiment the flow cell was disassembled, the fiber tip was wiped with ethanol and immersed in a vial containing distilled-deionized water, and the background fluorescence (B_2) was measured. The fiber tip was then immersed into a vial containing 400 μg/mL water-soluble fluorescein (Sigma) and a second fluorescence spectrum (S_2) was collected. Fluorescence attributed to the water-soluble fluorescein was the difference between the fluorescein solution signal and the water background ($F_2 = S_2 - B_2$). Since each experiment necessitated an individually prepared sensing tip, and since several different fiber probes were employed, the raw avidin signal intensity collected with each sensor F' was normalized with the corresponding value of F_2 determined at the end of each experiment. All fluorescence data presented in this paper were normalized in this fashion (i.e. $F = F'/F_2$) and thus reported in relative intensity units.

Results

Avidin Binding to Sensor Tip. Thirty three different LB affinity surfaces (16 for B-DPPE, 16 for B-X-DPPE, and an AA control) were deposited on a series of silanized EFO sensor tips as presented in Table I. In general, the fluorescence intensity collected at 515 nm increased as FITC-avidin bound to the sensor surface, eventually leading to a saturation asymptote. The fluorescence intensity at saturation increased with increasing doping density of the biotin receptor (Figure 2), and for a given doping density, the chain extended B-X-DPPE lipid bound

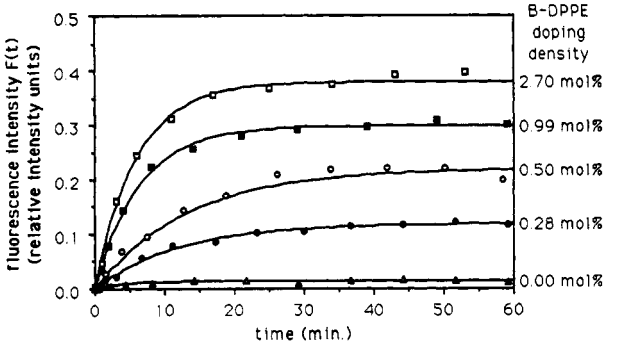

Figure 2. Time-dependent increase of fluorescence intensity as FITC-avidin binds to the sensor tip. Note that the saturation asymptote increases with increasing doping density of B-DPPE at the sensor tip. Solid lines are best fit of the time-dependent fluorescence data to the bimolecular reaction model.

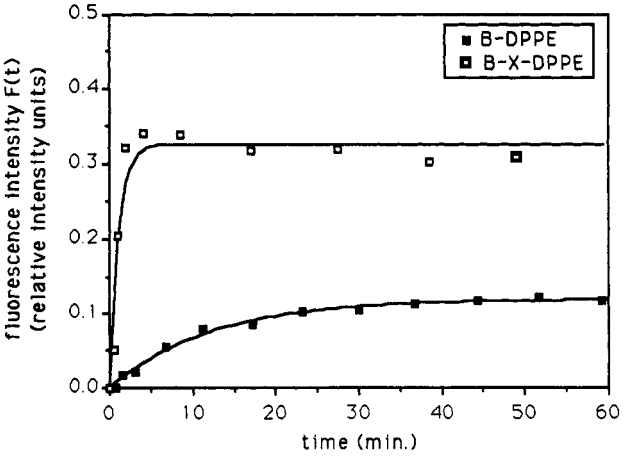

Figure 3. Time-dependent increase of fluorescence intensity for sensor tips doped with 0.28 mol % B-DPPE and B-X-DPPE. Note that the more accessible B-X-DPPE biotin lipid bound a greater amount of FITC-avidin and reached its saturation asymptote in a shorter time period than did B-DPPE.

greater amounts of avidin in a shorter time period than did B-DPPE (Figure 3).

By employing a bimolecular reaction model described in Appendix A, the fluorescence intensity from FITC-avidin bound to the sensor surface can be expressed as a function of time

$$F(t) = F_e[1 - \exp(-t/\beta)] \quad (1)$$

where F_e is the fluorescence intensity when the binding reaction reaches equilibrium and β is the characteristic time constant corresponding to the time for $F(t)$ to reach 63.2% [$100(1-e^{-1})$] of its equilibrium value F_e. The solid lines in Figures 2 and 3 are best fits of the time-dependent data to eq 1 determined by using a nonlinear least-squares routine.

Table II lists the values F_e and β obtained from the least-squares fitting of eq 1 to the time-dependent avidin binding experimental data. These data (Figures 2 and 3 and Table II) suggest that (1) a surface doped with B-X-DPPE binds more avidin at equilibrium than does the corresponding surface doped with B-DPPE and (2) increasing the biotin doping density causes the avidin binding to proceed more quickly for B-DPPE and slow down for B-X-DPPE.

Avidin Desorption from Sensor Tip. Prior to the initiation of the desorption measurements, avidin was first allowed to bind to the sensor surface until equilibrium was achieved. Then the desorption measurements were initiated by replacing the avidin solution with a highly

Table II. Fitted Parameters from Biomolecular Reaction Model of Avidin Binding to Sensor Tip

biotin lipid doping density (mol %)	equilibrium fluorescence intensity F_e (10^{-2} relative intensity units)[a]		characteristic time constant $1/\beta$ (10^{-3} s^{-1})[b]	
	B-DPPE	B-X-DPPE	B-DPPE	B-X-DPPE
0.00	1.37 ± 0.10	1.37 ± 0.10	4.50 ± 1.50	4.50 ± 1.50
0.17		10.0 ± 0.43		11.9 ● 1.80
0.28	11.9 ± 0.16	25.8 ± 0.90	1.39 ± 0.07	12.7 ● 1.86
0.40	18.5 ± 0.43	35.1 ± 1.18	0.84 ± 0.07	9.20 ± 1.28
0.50	19.3 ± 073	34.6 ± 1.32	1.71 ± 0.23	8.46 ● 1.25
0.63	27.6 ± 0.61	53.2 ± 2.01	1.75 ± 0.15	7.19 ± 1.09
0.76	29.4 ± 0.64	32.1 ± 0.52	1.41 ± 0.12	6.44 ± 0.41
0.99	30.0 ± 0.30	40.2 ± 0.73	2.59 ± 0.11	5.13 ± 0.33
1.41	27.1 ± 0.25	31.9 ± 0.84	1.86 ± 0.08	5.06 ● 0.49
1.79	27.4 ± 0.39	42.8 ± 0.93	2.26 ± 0.13	5.25 ± 0.42
2.17	32.1 ± 0.74	40.1 ● 1.02	3.50 ± 0.32	5.65 ± 0.59
2.70	38.1 ± 0.37		2.79 ± 0.13	
3.23	40.8 ± 1.01	57.6 ± 0.80	3.69 ± 0.45	4.05 ± 0.18
4.76	36.3 ± 0.83		4.31 ± 0.43	
6.25	46.5 ± 0.61	56.0 ± 2.19	2.23 ± 0.12	4.20 ± 0.49
16.7	38.7 ± 0.86	67.5 ± 0.97	4.61 ± 0.45	2.91 ● 0.25
100	46.9 ± 0.41	65.6 ± 0.12	3.32 ± 0.15	2.72 ± 0.16

[a] ±standard deviation of least-squares fit F_e. [b] ±standard deviation to β.

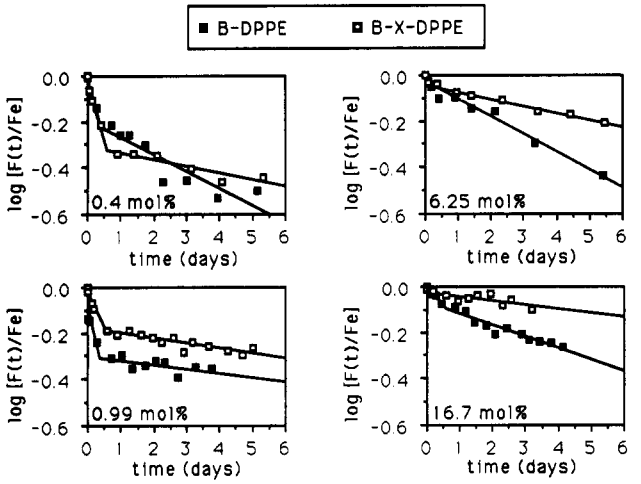

Figure 4. Semilog plots of FITC-avidin desorbing from fiber tips doped with 0.4, 0.99, 6.25, and 16.7 mol % B-DPPE and B-X-DPPE. The solid lines represent the linear best fits of the data for short desorption times ($t < 0.5$ day) and longer desorption times ($t > 0.5$ day).

concentrated biotin solution. The excess of free biotin ensured that the accessible binding sites of an avidin molecule were immediately occupied with biotin from solution, thus preventing the rebinding of desorbed avidin to the sensor surface. The time course of avidin desorption was very slow and each experiment was conducted for a minimum of 4 days. Therefore, only eight sensor tips were examined, each doped with B-DPPE or B-X-DPPE at either 0.40, 0.99, 6.25, or 16.7 mol % (denoted by † in Table I).

As discussed in Appendix B, the fluorescence from FITC-avidin bound on the sensor surface is described by an exponential function

$$F(t) = F_e \exp(-k_{-1}t) \quad (2)$$

where $F(t)$ is the normalized fluorescence intensity, F_e the initial fluoresence intensity at the onset of the experiment, and k_{-1} the dissociation rate constant. Figure 4 contains plots of the time-dependent fluorescence decay observed as avidin desorbed from the sensor surface. These data are presented as log $[F(t)/F_e]$ vs time where from eq 2

Table III. Dissociation Constant from Avidin Desorption from Sensor Tip

biotin lipid doping density (mol %)	dissociation constant k_{-1} (10^{-7} s^{-1})[a]			
	B-DPPE		B-X-DPPE	
	$t < 0.5$ day	$t > 0.5$ day	$t < 0.5$ day	$t > 0.5$ day
0.40	60.4 ± 12	8.5 ± 1.7	58.9 ± 11	3.3 ± 0.8
0.99	74.1 ± 41*	2.0 ± 0.9†	36.0 ± 4.7	2.6 ± 0.4
6.25	30.7 ± 2.8	8.9 ± 0.7	11.9 ± 6.7§	3.5 ± 0.2
16.70	19.6 ± 0.8	5.7 ± 0.6	6.8 ± 1.5	2.1 ± 1.0#

[a] ±standard deviation calculated from standard deviation of best fit to slope. Student's t test of slope: *, $p = 0.18$; §, $p = 0.21$, †, $p = 0.07$; #, $p = 0.08$; $p < 0.05$ for all other data.

$$\log [F(t)/F_e] = -(k_{-1}/2.303)t \quad (3)$$

where $-k_{-1}/2.303$ is the slope of the semilog desorption data. The solid lines in Figure 4 are linear best fits of eq 3 to the desorption data for $t < 0.5$ day and $t > 0.5$ day. From Figure 4 it appears that desorption occurred at a more rapid rate in the first 12 h for lower biotin-doped surfaces (0.4 and 0.99 mol %), whereas desorption proceeds at a nearly constant rate throughout the entire measurement period for higher biotin-doped surfaces (6.25 and 16.7 mol %).

Calculation of Dissociation and Association Rates. Table III contains the dissociation rate constants of the surface-bound avidin/biotin complex determined from the desorption data in Figure 4 via linear least-squares fits to eq 3. For a given doping density, the general trends in the desorption data in Table III are as follows: (1) the dissociation rates are consistently higher for short desorption times ($t < 0.5$ day) than for longer desorption times ($t > 0.5$ day), particularly for the lower doping densities (i.e. 0.4 and 0.99 mol %); (2) the dissociation rates were generally higher for B-DPPE than for B-X-DPPE (the exceptions being 0.4 mol % at $t < 0.5$ day and 0.99 mol % at $t > 0.5$ day). Note that most of the dissociation rates in Table III are considerably higher than that reported by Green (0.9×10^{-7} s^{-1}) for avidin/biotin dissociation in solution.[17]

From the magnitudes of k_{-1} in Table III and β in Table II, it is clear that $k_{-1}\beta \ll 1$. Therefore, we obtain from eq A5c of Appendix A

$$k_{+1} \approx (\beta[A]_0)^{-1} \quad (4)$$

where k_{+1} is the association rate constant, β is the characteristic time constant, and $[A]_0$ is the initial avidin solution concentration.

Table IV contains values of k_{+1} calculated from the avidin binding data in Table II via eq 4. For these calculations, $[A]_0 = 149$ nM (10 μg/mL) for avidin binding to B-DPPE and $[A]_0 = 74.5$ nM (5 μg/mL) for avidin binding to B-X-DPPE (see Experimental section). Figure 5 is a semilog plot of the association rates in Table IV vs mol % biotin lipid doping density. From these data it is clear that surfaces doped with B-DPPE and B-X-DPPE converge to nearly the same value of k_{+1} for doping densities greater than 10 mol %, but from opposite directions. Therefore, increasing the biotin lipid doping density progressively hastens the binding of avidin to B-DPPE but progressively inhibits the binding of avidin to B-X-DPPE. However, after approximately 10 mol %, both the B-DPPE and B-X-DPPE doped surfaces appear to bind avidin with similar facility. Also note that all of the association rates in Table IV and Figure 5 range from 3

Table IV. Association Constants from Avidin Binding to Sensor Tip

biotin lipid doping density (mol %)[a]	association constant k_{+1} (10^4 M^{-1} s)[b]	
	B-DPPE	B-X-DPPE
0.00	3.02 ± 1.01	6.04 ± 2.01
0.17		15.97 ± 2.42
0.28	0.93 ± 0.47	17.05 ± 2.50
0.40†	0.56 ± 0.05	12.35 ± 1.72
0.50	1.15 ± 0.15	11.36 ± 1.68
0.63	1.17 ± 0.10	9.65 ± 1.55
0.76	0.95 ± 0.08	8.64 ± 0.55
0.99†	1.74 ± 0.07	6.88 ± 0.44
1.41	1.25 ± 0.05	6.79 ± 0.66
1.79	1.52 ± 0.09	7.05 ± 0.56
2.17	2.35 ± 0.22	7.58 ± 0.79
2.70	1.87 ± 0.09	
3.23	2.48 ± 0.30	5.44 ± 0.24
4.76	2.89 ± 0.29	
6.25†	1.50 ± 0.08	5.64 ± 0.69
16.70†	3.09 ± 0.30	3.91 ± 0.34
100.00	2.23 ± 0.10	3.65 ± 0.22

[a] † indicates doping densities used in both binding and desorption experiments. [b] ± (standard deviation of least-squares best fit to β divided by $[A]_0$).

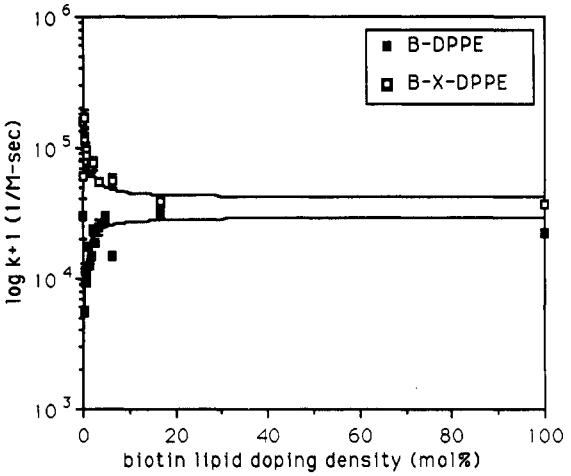

Figure 5. Semilog plot of avidin association constants of binding to the sensor tip plotted as a function of biotin lipid doping density. Note that the association rates converged to nearly the same value with increased doping densities of B-DPPE and B-X-DPPE, but from opposite directions.

to 4 orders of magnitude slower than that reported by Green (1.5×10^8 M^{-1} s) for avidin/biotin association in solution.[17]

Discussion

From several recent reports,[19-25] it appears that the binding affinity of protein ligands to receptor-doped lipid surfaces is significantly affected by the protein solution concentration and receptor density in the membrane as well as the accessibility of the receptor to the ligand at the lipid surface. However, Kalb et al. did not alter the accessibility of the receptor to the antibody,[21] and Ringsdorf and co-workers did not vary the receptor density.[19,20] To our knowledge, only the study of Timbs et al.[25] varied both of these parameters and showed good correspondence between the amount of surface bound antibody and the receptor density. However, they observed no appreciable effect of hapten accessibility on the amounts of antibody bound to LB films of fluidlike lipids, and the equilibrium amounts of surface bound antibody was essentially negligible at doping densities lower than 5 mol %.

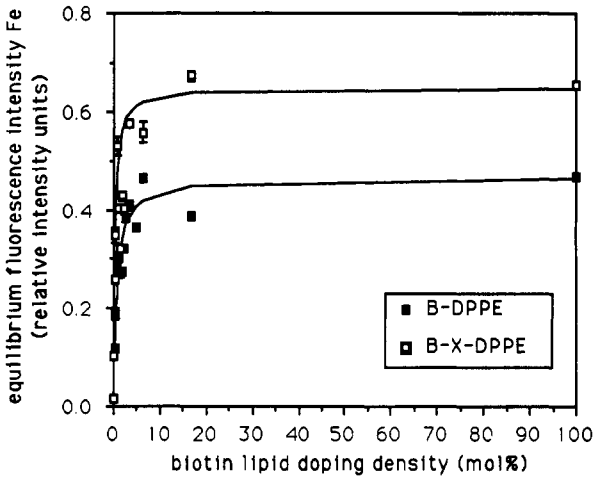

Figure 6. Equilibrium fluorescence intensity (e.g. saturation asymptote) of FITC-avidin bound to the sensor tip plotted as a function of biotin lipid doping density. Note that for the same doping density, B-X-DPPE bound more FITC-avidin at equilibrium than did B-DPPE. Solid lines are best fits of data to a Langmuir binding isotherm.

In this paper we have attempted to simultaneously address the issues of receptor density and receptor accessibility using a relatively rigid fatty acid monolayer as the matrix lipid. These measurements were performed using evanescent fiber optic (EFO) fluorescence spectroscopy to monitor the binding of avidin to a series of biotin-doped LB films deposited at the fiber tip. The LB films were doped from 0 to 100 mol % with one of two biotin lipids, either B-DPPE or a chain extended B-X-DPPE. As illustrated in Figure 1, these two biotin lipids are presumed to have their hapten groups just barely (B-DPPE) and completely (B-X-DPPE) protruding above the AA head groups.

Figure 6 is a plot of the equilibrium FITC-avidin fluorescence intensities at receptor saturation (F_e) listed in Table II. These data show a series of hapten-doped surfaces that bind increasing amounts of protein with increasing doping density until about 5 mol % doping. Beyond 5 mol % the surfaces appeared to become crowded with avidin, and further increases in doping density had little effect on the LB film's ability to accommodate more protein. Therefore, unlike the work of Timbs et al.,[25] the most sensitive modulation of receptor-dependent avidin

(19) Ahlers, M.; Grainger, D. W.; Herron, J. N.; Lim, K.; Ringsdorf, H.; Salesse, C. Quenching of Fluorescein-Conjugated Lipids by Antibodies: Quantitative Recognition and Binding of Lipid-Bound Haptens in Biomembrane Models, Formation of Two Dimensional Protein Domains and Molecular Dynamic Simulations. *Biophys. J.* **1992**, *63*, 823–838.

(20) Blankenberg, R.; Meller, P.; Ringsdorf, H.; Salesse, C. Interaction Between Biotin Lipids and Strepavidin Monolayers: Formation of Oriented Two-Dimensional Protein Domains Induced by Surface Recognition. *Biochemistry* **1989**, *28*, 8214–8221.

(21) Kalb, E.; Engel, J.; Tamm, L. K. Binding of Proteins to Specific Target Sites in Membranes Measured by Total Internal Reflection Fluorescence Microscopy. *Biochemistry* **1990**, *29*, 1608–1613.

(22) Pisarchick, M. L.; Thompson, N. L. Binding of a Monoclonal Antibody and its Fab Fragment to Supported Phospholipid Monolayers Measured by Total Internal Reflection Fluorescence Microscopy. *Biophys. J.* **1990**, *58*, 1253–1249.

(23) Poglitsch, C. L.; Thompson, N. L. Interaction of Antibody with Fc Receptors in Substrate-Supported Planar Membranes Measured by Total Internal Reflection Fluorescence Microscopy. *Biochemistry* **1990**, *29*, 248–254.

(24) McConnell, H. M.; Watts, T. H.; Weis, R. M.; Brian, A. A. Supported Planar Membranes in the Study of Cell-Cell Recognition in the Immune System. *Biochim. Biophys. Acta* **1986**, *846*, 95–106.

(25) Timbs, M. M.; Poglitsch, C. L.; Pisarchick, M. L.; Sumner, M. T.; Thompson, N. L. Binding and Mobility of Anti-Dinitrophenyl Monoclonal Antibodies on Fluid-Like, Langmuir-Blodgett Phospholipid Monolayers Containing Dinitrophenyl-Conjugated Phospholipids. *Biochim. Biophys. Acta* **1991**, *1064*, 219–228.

Table V. Apparent Affinity Constant of Avidin for the Biotin-Doped Sensor Tip

biotin lipid doping density (mol %)	apparent affinity constant K_a (10^{10} M^{-1})[a]			
	B-DPPE		B-X-DPPE	
	$t < 0.5$ day	$t > 0.5$ day	$t < 0.5$ day	$t > 0.5$ day
0.40	0.09 ± 0.02	0.67 ± 0.1	2.10 ± 0.5	37.20 ± 10.0
0.99	0.24 ± 0.1*	8.56 ± 4.0*	1.91 ± 0.3	26.77 ± 4.6
6.25	0.49 ± 0.1	1.69 ± 0.2	4.74 ± 2.7*	16.25 ± 2.3
16.70	1.58 ± 0.2	5.48 ± 0.8	5.77 ± 1.4	18.51 ± 9.1*

[a] ± cumulative standard deviation calculated from Tables III and IV. The asterisk indicates a Student's t test of k_{-1} used to calculate K_a:$p > 0.05$ (see Table II).

binding to the sensor tip occurred at doping densities of less than 5 mol %. The solid lines in Figure 6 are the best fits of these data to a Langmuir binding model obtained from reciprocal plots of the F_e values in Table II (not shown). This analysis yielded apparent affinity constants of $K_a = 3.71 \times 10^{11}$ cm²/mol (±7%) for B-X-DPPE and $K_a = 1.51 \times 10^{11}$ cm²/mol (±9%) for B-DPPE (Student's t tests of slope and intercept: $p < 0.05$). Therefore, similar to the observations of Ringsdorf and co-workers,[19,20] avidin bound with greater affinity to fiber surfaces doped with the more accessible B-X-DPPE than it did to fibers doped with the less accessible B-DPPE.

In general, the time course of the avidin binding data was well fit by a simple bimolecular reaction model described by eq 1, while the fit of eq 3 to the desorption data was less satisfying, with two fits judged insignificant at the 95% confidence level and two fits judged insignificant on the 90% confidence level (Table III). However, inspection of Figure 4 shows a clear trend of higher desorption rates at early times, particularly for the lower doping densities. Therefore, it appears that avidin binding follows pseudo-first-order rate kinetics, while the higher dissociation rate at shorter desorption times indicates that avidin desorption is more complex. Furthermore, increasing the doping density decreased the rate of avidin desorption at early times from both biotin lipids (Table III and Figure 4), but it had nearly opposite effects on avidin binding to B-X-DPPE and B-DPPE (Table IV and Figure 5). In addition, our association rates are orders of magnitude lower, and our dissociation rates are considerably higher, than that reported by Green for avidin/biotin binding in solution.[17] Green similarly reported higher dissociation rates in the early stages of avidin/biotin dissociation in solution and in the dissociation of avidin subunits polymerized by bifunctional biotin linkers.[26] He also observed that avidin would not form stable polymer until the biotin linkers reached a critical length, suggesting a biotin linker bound to one avidin could not be bound by a second avidin unless it was sufficiently accessible.

Table V and Figure 7 contain the apparent association constants (K_a) calculated for avidin binding to the biotin-doped LB films for which both binding and dissociation measurements were performed. These affinity constants were calculated via the relationship

$$K_a = k_{+1}/k_{-1} \quad (5)$$

where k_{-1} and k_{+1} are listed in Tables III and IV, respectively. Note that all of the calculated association constants range from 4 to 6 orders of magnitude lower than the association constant of 1.6×10^{15} M^{-1} reported by Green for avidin/biotin binding in solution.[17] Figure 7 suggests an affinity of avidin for the sensor surface that, for a given biotin surface density, increases with both biotin

(26) Green, N. M. Avidin. *Adv. Protein Chem.* **1975**, *29*, 85–133.

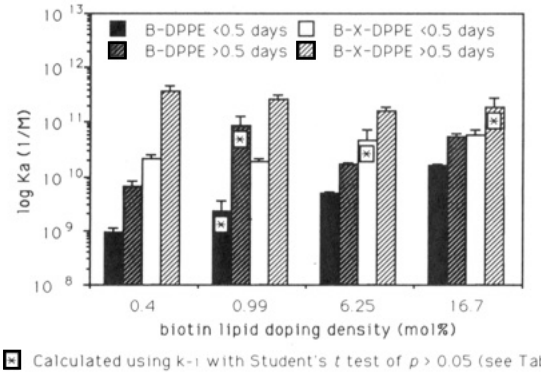

Figure 7. Apparent affinity constants calculated for biotin doping densities used in both FITC-avidin binding and desorption experiments. Note that with the exception of B-DPPE at $t >$ 0.5 day, there is a trend of increased binding affinity at longer desorption times and increased biotin accessibility, with these effects being most pronounced at lower doping densities.

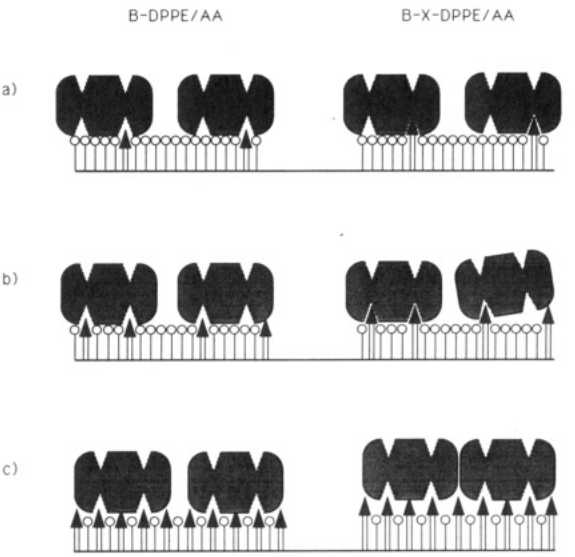

Figure 8. Illustration of avidin binding to sensor surfaces doped with B-DPPE and B-X-DPPE at low (a), intermediate (b), and high (c) doping densities.

accessibility and desorption time. The only exception to this trend is the affinity of avidin for 0.99 mol % B-DPPE at $t > 0.5$ day. At least qualitatively, these data agree with the Langmuir analysis of the data in Figure 6.

To a first approximation, our results can be explained by considering the combined influence of biotin lipid surface density , biotin accessibility, surface crowding of biotin-bound avidin molecules, and monovalently vs bivalently bound avidin. Other influences, such as biotin lipid aggregation, membrane fluidity, protein conformational changes, nonideal avidin binding, and variations in the quantum efficiency of the fluorescent label are possible contributors, but their impact appears to have been minor in comparison.

Figure 8 is an illustration of what we speculate is occurring at the sensor surface. In general, at low doping densities (e.g. 0–1 mol %) the biotin lipids are isolated and avidin binds more readily to B-X-DPPE than it does to B-DPPE (Figure 8a). However, the biotin surface density is so low that binding remains primarily monovalent. Therefore, much of the avidin is relatively loosely bound and desorbs quickly, resulting in a distribution of binding affinities that is on the average higher for B-X-DPPE than it is for B-DPPE. At intermediate doping densities (e.g. 1–10 mol %), the reduced space between biotin lipids increases avidin binding to the less accessible

B-DPPE, while the increased crowding of biotin lipids decreases the accessibility of the chain extended B-X-DPPE and inhibits avidin binding (Figure 8b). But early desorption of avidin does not decrease until the doping density is high enough to allow sufficient bivalent avidin binding [e.g. early desorption remains high for 0.99 mol % (~2 biotins/avidin) and is reduced for 6.25 mol % (~10 biotins/avidin)]. At higher doping densities (e.g. >10 mol %) much more of the surface is populated with biotin lipid and avidin binds at a roughly equivalent rate to both B-X-DPPE and B-DPPE because the biotin lipids are no longer sufficiently isolated to be differentially accessible (Figure 8c). The doping density is now high enough that the majority of avidin molecules will eventually bind a second biotin lipid, thus reducing the level of avidin desorption at early times.

Conclusions

Our results suggest an overall trend of sterically hindered binding of avidin to the biotin lipids at the sensor surface. In comparison to relatively unconstrained biotin binding in solution, avidin appears to have greater difficulty accommodating the biotin hapten at the sensor surface into the binding site, resulting in drastically reduced association rates of avidin binding to the sensor surface and consistently higher dissociation rates for avidin desorption from the sensor surface. Receptor accessibility and receptor density appeared to have similar effects on increasing the level of avidin binding to the sensor surface. However, higher receptor densities reduced the rate of avidin desorption at early times, presumably through an increased incidence of bivalent binding, whereas the impact of receptor accessibility on the rate of avidin binding was quickly diminished with increasing receptor density, probably because the biotin lipids become encumbered by the effects of receptor crowding.

Appendix A: Avidin Binding

If one assumes that protein–protein interactions are absent, the binding of avidin (A) to a surface with biotin receptors (B) can be considered approximately as a reversible bimolecular reaction

$$A + B \underset{k_{-1}}{\overset{k_{+1}}{\rightleftharpoons}} AB \tag{A1}$$

where A, B, and AB are free avidin, unbound biotin, and avidin-bound biotin, respectively, and k_{+1} and k_{-1} are the first-order association and dissociation rate constants of the reaction.

According to first-order kinetics, the rate of formation of AB complex in a bimolecular reaction is given by

$$d[AB]/dt = k_{+1}[A][B] - k_{-1}[AB] \tag{A2}$$

where [A] is the concentration of avidin in solution, [B] is the surface density of vacant biotin receptors, and [AB] is surface density of the avidin–biotin complex. Since the total number of biotin receptors is conserved, and the number of avidin molecules in the solution is much larger than the number of available surface binding sites, we have

$$[B] = [B]_0 - [AB] \tag{A3a}$$

$$[A] \approx [A]_0 \tag{A3b}$$

where $[A]_0$ and $[B]_0$ are the initial avidin solution concentration and biotin receptor surface density, respectively. From eqs A2, A3a, and A3b we obtain the time-dependent increase in the formation of the avidin–biotin complex

$$[AB](t) = [AB]_e[1 - \exp(-t/\beta)] \tag{A4}$$

where

$$[AB]_e = \alpha\beta \tag{A5a}$$

$$\alpha = k_{+1}[A]_0[B]_0 \tag{A5b}$$

$$1/\beta = k_{+1}[A]_0 + k_{-1} \tag{A5c}$$

$[AB]_e$ in eq A4 is the surface density of the avidin–biotin complex at equilibrium and β is the characteristic time constant corresponding to the time for [AB] to reach 63.2% of its equilibrium value.

Finally, if one assumes that the fluorescence intensity measured with the EFO sensor scales linearly to the amount of avidin bound to the surface, we may write

$$F(t) = \gamma[AB](t) \tag{A6}$$

where $F(t)$ is the normalized fluorescence intensity (see Experimental section) and γ is a scaling factor equal to the sensitivity of the sensor in units of fluorescence intensity per unit surface density of the avidin–biotin complex (i.e. intensity/(molecule/cm^2)). Therefore, from eqs A4 and A6, we obtain the time-dependent fluorescence expression

$$F(t) = F_e[1 - \exp(-t/\beta)] \tag{A7}$$

where F_e is the fluorescence intensity at equilibrium given by

$$F_e = \gamma[AB]_e \tag{A8}$$

Appendix B: Avidin Desorption

As discussed in the main text, a biotin solution of high concentration was used in the desorption experiments to eliminate the rebinding of dissociated avidin to the sensor surface. If one assumes that the presence of excess free biotin rendered the process of avidin dissociation irreversible (i.e. $k_{+1} = 0$), then the expression for avidin desorption from the sensor surface is easily obtained from eq A2

$$d[AB]/dt = -k_{-1}[AB] \tag{B1}$$

where k_{-1} is the first-order dissociation rate constant. The solution to eq B1 is an simple exponential function

$$[AB](t) = [AB]_e \exp(-k_{-1}t) \tag{B2}$$

where for our experimental setup $[AB]_e$ is the surface density of avidin prior to the initiation of desorption. Invoking the same assumptions implicit in eq A8, we obtain the expression for the time-dependent fluorescence decay caused by avidin desorption from the sensor surface

$$F(t) = F_e \exp(-k_{-1}t) \tag{B3}$$

where F_e is the fluorescence intensity measured at the initiation of the desorption experiment.

Acknowledgment. This work was funded by a biomedical research grant from the Whitaker Foundation, NIH Grant HL 32132, and a graduate fellowship from the NSF/ERC Center for Emerging Cardiovascular Technologies (S.Z.). Special appreciation is extended to Dr. G. A. Truskey of Duke University for his keen assistance in the statistical analysis of our experimental results.